27 Apr 1981, 2:00 pm - 5:00 pm

Mechanical Behavior of Granite Under Cyclic Compression

V. Rajaram

E. K. Lehmann & Associates, Inc., Minneapolis, MN

Proceedings: First International Conference on Recent Advances in Geotechnical Earthquake Engineering and Soil Dynamics, April 26 - May 3, 1981, St. Louis, Missouri

Mechanical Behavior of Granite Under Cyclic Compression

V. Rajaram
Mining Engineer, E. K. Lehmann & Associates, Inc., Minneapolis, Minnesota

SYNOPSIS A better understanding of soil/rock-structure interaction is invaluable in the seismic design of concrete and masonry structures. In an effort to understand the behavior of rock under cyclic compression, both intact and faulted specimens of Westerly granite (2.5 cm. dia. x 6.25 cm. long) were subjected to uniaxial and triaxial loading at a uniform rate of one cycle per second. The fatigue strength under uniaxial loading at 10^6 cycles was found to be about 70% of the static compressive strength, and confining pressure improved fatigue resistance considerably. The accumulated permanent strain at the maximum stress level was found to be independent of the stress path and bounded by the complete stress-strain curve. Cyclic loading produces dilatancy and the stress at the onset of dilatancy is significantly reduced by repeated cycling. In faulted specimens (saw cut at 30 degrees to the longitudinal axis), the first loading cycle produces a large amount of sliding; subsequent cycles result in a decelerating rate of increase in the amount of sliding, with a steady-state equilibrium being reached in a few cycles. Cyclic loading increases crack porosity, and progressive microcracking causes fatigue failure.

INTRODUCTION

The importance of soil/rock-structure interaction effects in the seismic design of concrete and masonry structures has been firmly established (Dezfulian, 1976). The response of rock to static loads resulting from the weight of overlying material and tectonic forces is fairly well understood. However, rock behavior under dynamic loads, which produce premature failure at stress levels lower than their strength under static conditions, is not fully understood.

Cyclic loads are imposed on rock structures by blasting pulses and earthquake accelerations. In order to obtain quantitative data on the effect of these cyclic loads on the mechanical behavior of rock, both intact and faulted specimens of Westerly granite (2.5 cm dia. and 6.25 cm. long) were subjected to uniaxial and triaxial cyclic compression. Internal changes within the specimen causing fatigue failure were studied by measuring the cyclic deformation and acoustic emission during the tests.

EXPERIMENTAL PROGRAM

A servo-controlled electro-hydraulic testing machine, MTS model 810, was used for the tests. A special jig, designed by Kim (1973) was used for the uniaxial cyclic compression tests. The lower platen is rigidly attached to the loading ram and the upper platen is threaded into the load cell. A swivel head mechanism in the upper platen assures good alignment of the specimen in the loading system. The longitudinal strain was determined from end-to-end specimen displacement measurement. Lateral strain was measured with two strain gages bonded horizontally to opposite sides of the specimen. The acoustic emission from the specimen was detected and recorded on a strip chart recorder using the Dunegan acoustic emission system.

Cyclic triaxial compression tests were performed in a triaxial cell whose cross-section is shown in figure 1. Two pistons, each 2.54 cm. in diameter, enter the cell (one at either end) and are connected by a yoke. This system allows the volume of oil in the cell, and thus the confining pressure, to remain approximately constant when the axial load is cycled. Confining pressure was applied to the specimen through a pressure generating system. The axial displacement was measured with two DCDT 250 transducers and lateral strain was measured with strain gages bonded to the specimen. The piezo-electric transducer of the acoustic emission system was attached to the outside of the cell.

A triangular loading program was used so that a constant rate of loading and unloading could be obtained during each cycle. A cyclic frequency of one cycle per second (cps) was used in most tests. The maximum number of cycles per test was kept at one million. Faulted (saw-cut) specimens were prepared by cutting cylinders at 30 degrees to the longitudinal axis. The saw-cut faces were lapped with a 150 grit abrasive powder and cleaned to produce a uniform finish. Tygon tubing was used to facilitate holding the saw-cut specimen together during test setup.

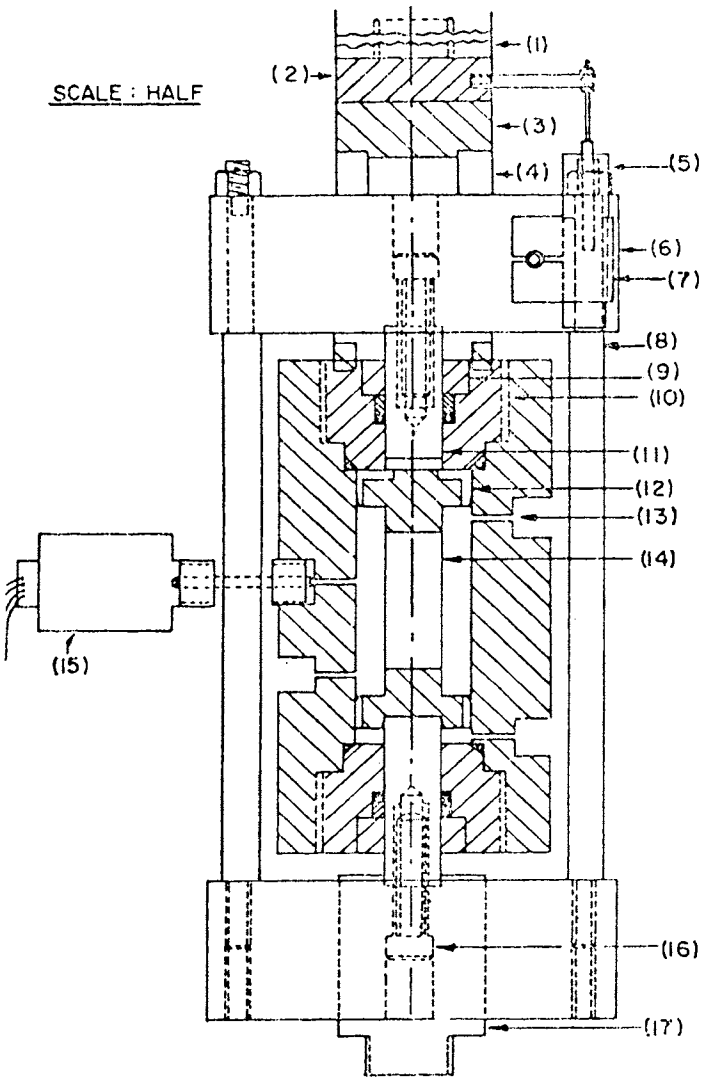

1. Load cell
2. Load cell adaptor
3. Pressure block
4. Extender
5. DCDT transducer
6. Yoke bar
7. Mounting block
8. Yoke rod
9. Compression nut
10. Upper nut
11. Upper piston
12. Upper platen
13. Oil outlet port
14. Rock specimen
15. Pressure transducer
16. Piston attaching screw
17. Ram adaptor

Figure 1. Cross-Section of Triaxial Cell

RESULTS

Intact Rock, Constant Maximum Stress

In these tests, the lower peak stress was kept constant at 1.4 MPa and the upper peak stress was kept constant during a test, but varied from test to test. The monotonic compressive strength obtained at a loading rate equivalent to one cycle per second was considered the 100% stress level. Subsequently, the upper peak stress was decreased in steps of 5% or less until no failure occurred in one million cycles. The number of cycles to failure at each stress level was determined.

The results of these experiments were plotted in terms of the ratio of the applied stress to the monotonic compressive strength(S) versus the logarithm of the number of cycles to failure (N). The S-N curve representing the increase in the number of cycles to failure with the reduction in the maximum stress level is presented in figure 2. The fatigue strength at one million cycles is 60% and 73% of the dynamic and static strengths, respectively. Table 1 summarizes the static, dynamic, and fatigue strengths, and the ratios of the fatigue to the static and dynamic strengths.

The effect of confining pressure is to increase the strength of granite and render it more resistant to fatigue failure. The fatigue strengths given above could be used as the effective compressive strength of intact rock in the design of structures which would be subjected to static, dynamic and cyclic loads. In addition, the weakening of the rock due to natural fractures has to be considered.

Accumulated strain during cycling, or cyclic creep, at both the minimum and maximum stress levels indicates three distinct stages: primary, steady-state, and tertiary (figure 3). This behavior is similar to that seen in static creep testing of rock (Jaeger and Cook, 1969). When the ratio of maximum stress level to the dynamic compressive strength was high (over 75%), the steady-state stage was absent. The average values of cyclic creep at the maximum stress level are plotted in figure 4 (horizontal lines). Cyclic stress relaxation values derived from strain-controlled tests are the vertical lines in figure 4. The complete stress-strain curve, as obtained by Wawersik (1968), is also shown. The plot indicates that cyclic creep at different maximum stress levels is bound by the ascending and descending portions of the complete stress-strain curve.

The S-N curve is related to the post-failure behavior under monotonic compression, i.e., the descending portion of the complete stress-strain curve. Wawersik (1968) defines Westerly granite as a Class II rock. It has a positively sloping descending stress-strain curve in the top 25 to 30% which limits the cyclic creep to failure; hence, the fatigue life is limited to about 20 cycles. At about 70% of the compressive strength, there is a transition from a positive to a negatively sloping descending stress-strain curve. Thus, cyclic creep to failure is not limited and fatigue life increases by several orders of magnitude. This results in the unique S-N curve observed for Westerly granite.

The acoustic emission-time curve (figure 3) appears to be a reliable precursor of fatigue failure. Acoustic emission accumulates considerably faster in the tertiary stage than in the two previous stages, probably due to the rapid propagation and coalescence of microcracks prior to failure. The emission begins even before the strain reaches this final stage; hence, it is better than the strain-time curve as an indicator of fatigue failure.

TABLE I

STATIC, DYNAMIC AND FATIGUE STRENGTHS
AT DIFFERENT CONFINING PRESSURES

Confining Pressure (MPa)	Static Comp. Strength (MPa) (1.4 MPa/Sec.)	Dynamic Comp. Strength (MPa) (1 cps)	Fatigue Strength (MPa) (at 10^6 cycles)	Fatigue/Static Strength (%)	Fatigue/Dynamic Strength (%)
0	262	321	192	73	60
6.9	347	412	268	77	65
17.2	431*	485	315	73	65

* Loading rate of 2.8 MPa/sec. 1 MPa = 145 psi.

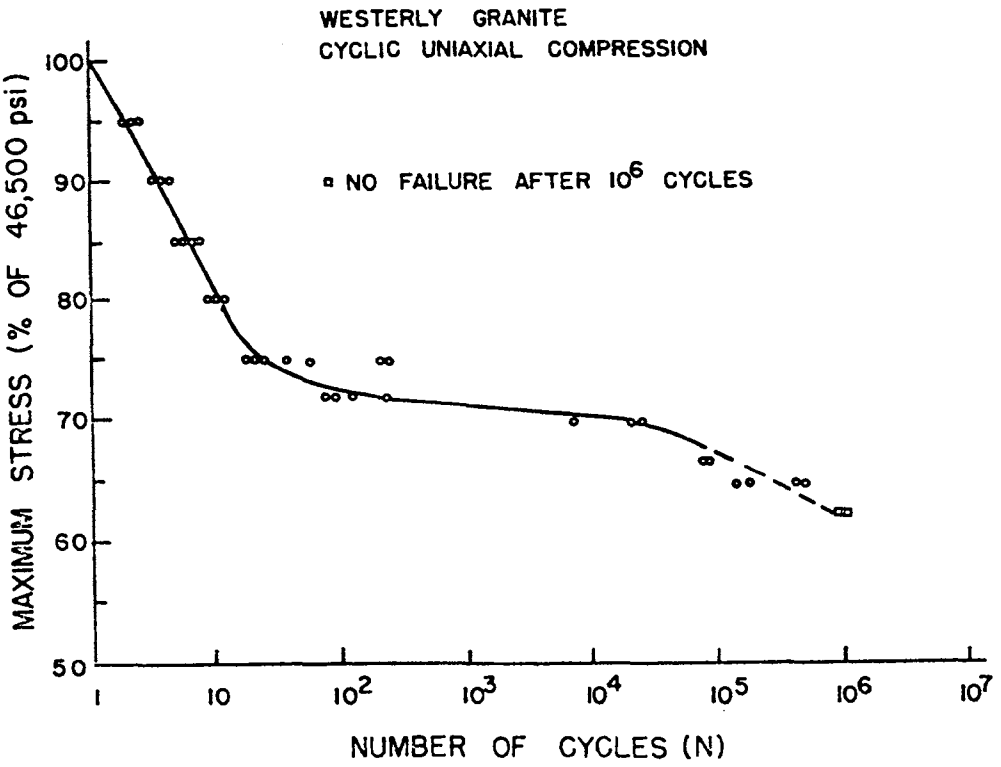

Figure 2. S-N Characteristics in Uniaxial Compression

The stress-strain curves (figure 3) show that the first cycle produces a large amount of permanent deformation, as verified by the distance between points O and A. During successive cycles, the rate of increase of permanent deformation becomes smaller and reaches a constant value. As failure approaches, the amount of permanent deformation increases at an accelerating rate. The cyclic creep at the maximum stress level develops faster than at the minimum stress level, resulting in a decrease of tangential modulus with cycling. The tangential modulus for the last cycle is 60.7 GPa compared to 71.7 GPa for the first cycle.

In some specimens, both axial and circumferential strains were measured. The circumferential strains accumulated at a faster rate than the axial strains, resulting in an increase of Poisson's ratio (measured at 50% of the upper peak stress) with cycling. In calculating Poisson's ratio for a cycle, the zero point was shifted to the origin of the coordinate system. Poisson's ratio increased from 0.26 for the first cycle to 0.87 for the last cycle. As failure approaches, Poisson's ratio becomes greater than 0.5 (the maximum value for an elastic continuum). This is probably due to the growth of axially oriented cracks with cycling.

Volumetric strains were computed with respect to the specimen volume before applying axial load. Typical stress-volumetric strain curves obtained for a specimen loaded to 75% of the dynamic compressive strength are presented in figure 5. The non-closure of the stress-volumetric strain loops indicates that the specimen volume increased at the end of each cycle. Since the stress-volumetric strain curves are continuously curved, the onset of dilatancy (defined as the stress at which the strain de-

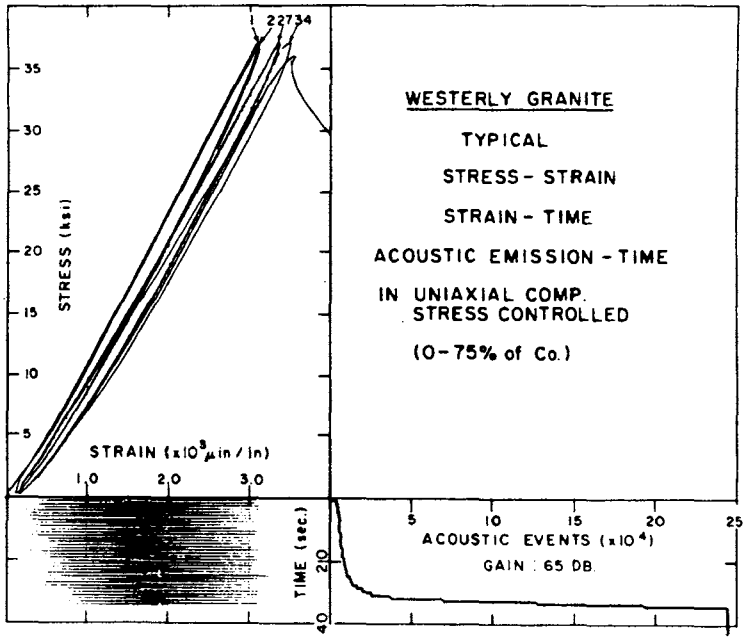

Figure 3. Typical Stress-Strain, Strain-Time, and Acoustic Emission-Time Curves in Uniaxial Compression

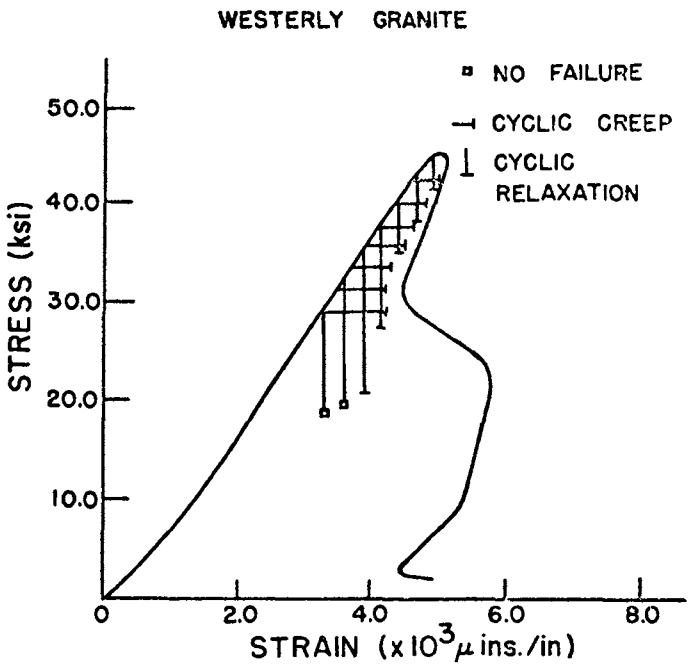

Figure 4. Upper Peak Cyclic Creep and Cyclic Stress Relaxation

parts from the linear or elastic portion of the stress-strain curve) is indiscernible, starting early in the loading history of each cycle. Although the onset of dilatancy is indiscernible in any given cycle, superimposing the stress-volumetric strain curves for the various cycles over each other indicates that there is a trend toward the progressive lowering of the onset of dilatancy. This demonstrates that the process of dilatant crack growth progresses with cycling and eventually produces specimen failure. Similar observations have been made by Scholz and Kranz (1974).

The reduction in the onset of dilatancy, the increase in Poisson's ratio, and the reduction in tangential modulus are not as pronounced under triaxial cyclic compression. The fatigue strength also increases under triaxial conditions (table I). This is due to the fact that the growth of axial (non-horizontal) cracks, which results in an increase of circumferential strain and Poisson's ratio, is suppressed by the application of confining pressure. The sliding along crack surfaces is inhibited, and flat cracks close due to the confining pressure. The increase of Poisson's ratio was from 0.21 for the first cycle to 0.43 for the last cycle, whereas in the uniaxial case the increase was from 0.26 to 0.87.

Intact Rock, Variable Maximum Stress

The cumulative damage and the loading path dependence in cyclic loading were studied by conducting a series of tests in which the maximum stress was varied after a certain number of cycles. In some tests the maximum stress was increased from one level to a higher one (lo-hi), and in others, the maximum stress was decreased from one level to a lower one (hi-lo).

A typical stress-longitudinal strain curve obtained in hi-lo tests is presented in figure 6. The amount of cyclic creep to failure was only a function of the last magnitude of the applied stress, and independent of the path taken to reach that value. Thus, independent of the loading path, whenever the cyclic stress-strain curve approaches or intersects the descending portion of the complete stress-strain curve, instability develops and the specimen fails

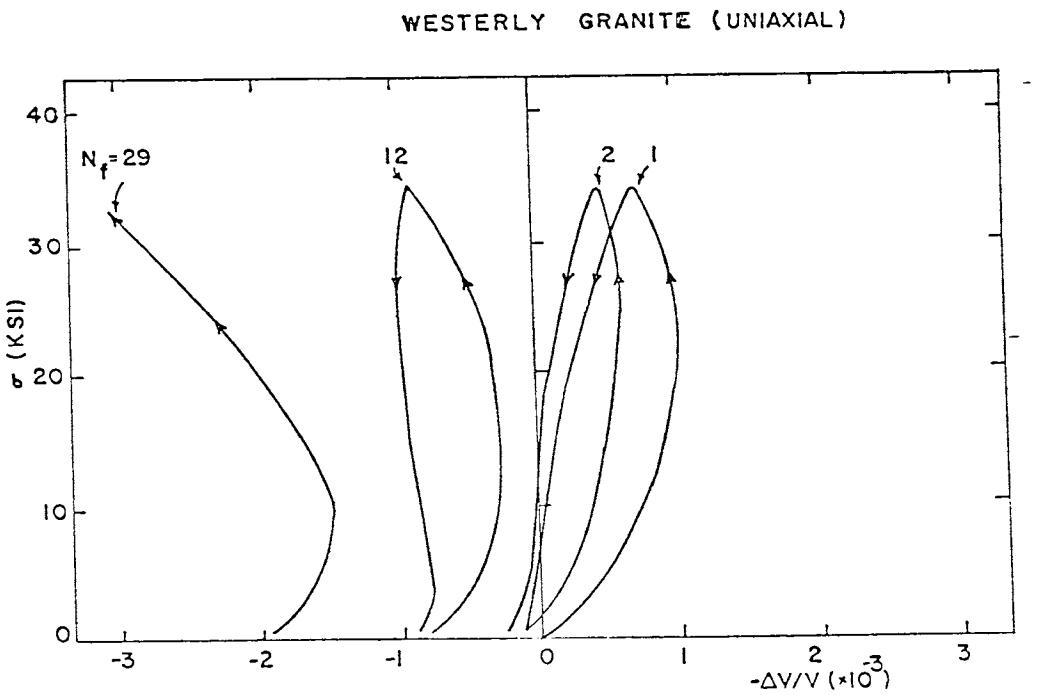

Figure 5. Typical Stress-Volumetric Strain Curves in Uniaxial Compression

(refer to figure 4).

The number of cycles to failure was significantly affected by the loading path used, thereby indicating the considerable effect that cumulative damage has on fatigue life of rock. For example, the fatigue life for a specimen loaded to a 65% maximum stress level is 465,300 cycles (figure 6). However, if the specimen is loaded to a stress level of 75% for 25 cycles and subsequently loaded to a 65% level, the fatigue life reduces to 7,850 cycles. This drastic reduction in fatigue life is due to the cumulative damage from loading at the 75% and 65% stress levels.

Saw-cut Rock: Variable Maximum Stress

Saw-cut specimens, having a cut at 30 degrees to the longitudinal axis, were tested monotonically at confining pressures of 6.9, 17.2, 34.5, and 55.2 MPa. Frictional strengths, i.e., the maximum stress that faulted rock can sustain beyond which it offers no frictional resistance, at these confining pressures are presented in table II.

Stress controlled cyclic tests were performed in which the axial stress level was cycled between 6.9 MPa and a maximum stress which was varied from test to test. Confining pressure was maintained at 6.9 MPa and the rate of cycling was one cycle per second. The amount of sliding was largest in the first cycle and gradually reduced in subsequent cycles, reaching a steady-state frictional equilibrium within a few cycles (usually 15 to 20). After frictional equilibrium was achieved, the maximum stress level was increased. This caused an increase of normal and shear stresses on the saw-cut, and produced renewed sliding. A typical stress-strain curve obtained in these tests is presented in figure 7.

In an attempt to understand this frictional equilibrium associated with cycling, the saw-cut specimens were carefully removed from the triaxial cell after the test and observed. It was found that this equilibrium was due to striations on the saw-cut faces and gouge (powdery material) build-up around the striations (figure

TABLE II

FRICTIONAL STRENGTHS OF SAW-CUT WESTERLY GRANITE AT VARIOUS CONFINING PRESSURES

Confining Pressure (MPa)	Loading Rate (MPa/sec)	Intact Rock Strength MPa	Frictional Strength MPa	Frictional Strength / Intact Rock Strength %	Coefficient of Friction
6.9	1.38	347	25.2	7.25	0.82
17.2	2.76	431	70.3	16.3	0.75
34.5	2.76	505	105.4	20.9	0.59
55.2	2.76	-	147.2	-	0.54

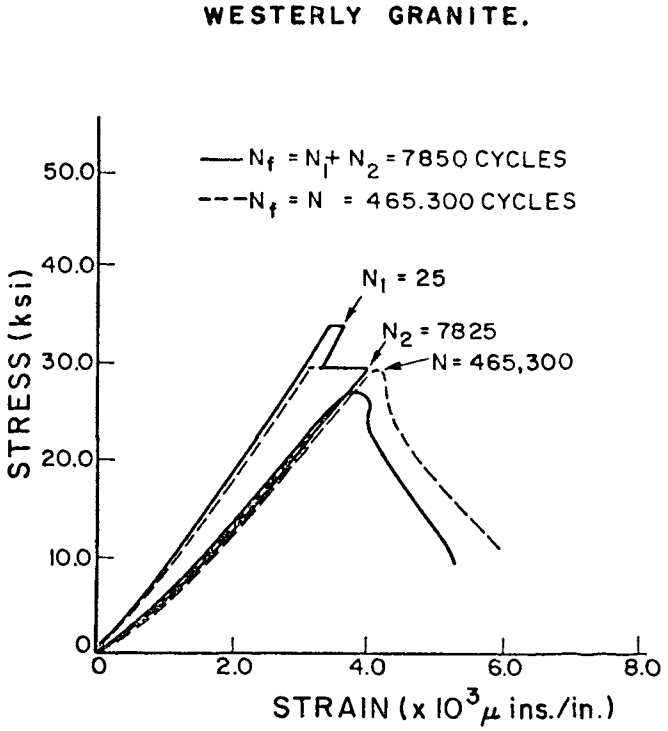

Figure 6. Path Dependence in Stress-Controlled Tests

8). The striations are apparently caused by an increase in true contact area along the saw-cut faces, and the gouge results from the crushing of asperities.

CONCLUSIONS AND PRACTICAL APPLICATIONS

1. The fatigue strength of rock as obtained in these tests should be used as the effective compressive strength of intact rock in the design of structures that may be subjected to static, dynamic and cyclic loads. The experimental results indicate that a value

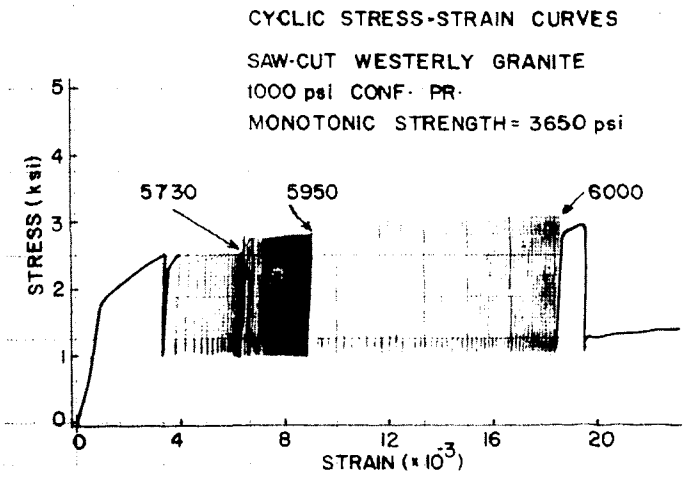

Figure 7. Typical Cyclic Stress-Strain Curves for Saw-Cut Rock

Figure 8. Saw-Cut Specimen Showing Striations and Gouge Buildup Due to Cyclic Loading

of 70% of the appropriate static strength would be a safe, effective uniaxial compressive strength for Westerly granite. Confining pressure increases produce corresponding increases in fatigue strength.

2. The complete stress-strain curve could be used to give an indication of the upper bound of the maximum allowable cyclic creep to failure, irrespective of the loading path utilized.

3. Acoustic emission monitoring can be used as an effective tool in predicting fatigue failure of rock.

REFERENCES

Dezfulian, H., 1976, Finite element analysis of seismic soil-structure interaction effects for nuclear power plants, Cento Seminar on Recent Advances in Earthquake Hazard Minimization, Teheran, 284-299.

Jaeger, J.C., and N.G.W., Cook, 1969, Time dependent effects, in Fundamentals of Rock Mechanics, Methuen and Co., Ltd., London, 513p.

Kim, C.M., 1973, Fatigue failure of rock in cyclic uniaxial compression, Ph.D. Thesis, UW, Madison, Wisconsin.

Scholz, C.H., and R., Kranz, 1974, Notes on dilatancy recovery, Journal of Geophysical Research, Vol. 79, No. 14, 2132-2135.

Wawersik, W.R., 1968, Detailed analysis of rock failure in laboratory compression tests, Ph.D. Thesis, University of Minnesota.

ACKNOWLEDGEMENTS

This paper represents a portion of the Ph.D. thesis of the author. The research was conducted under the guidance of Prof. B.C. Haimson and funded by the Advanced Research Projects Agency of the U.S. Department of Defense.